Title	Hybrid energy storage for energy harvesting powered wireless sensor networks
Author(s)	Wang, Wensi S.; Wang, Ningning; Hayes, Michael; O'Flynn, Brendan; Ó Mathúna, S. Cian
Publication date	2011-03
Original citation	Wang, Wensi S.; Wang, Ningning; Hayes, Michael; O'Flynn, Brendan; Ó Mathúna, S. Cian (2011) Hybrid energy storage for energy harvesting powered wireless sensor networks. Smart Systems Integration 2011. Dresden, Germany, 22-23 March, 2011.
Type of publication	Conference item
Link to publisher's version	http://www.vde-verlag.de/buecher/563324/smart-systems-integration-2011.html Access to the full text of the published version may require a subscription.
Rights	**© VDE VERLAG GMBH.**
Item downloaded from	http://hdl.handle.net/10468/533

Hybrid Energy Storage for Energy Harvesting Powered Wireless Sensor Networks

[1]Wensi Wang, [2]Ningning Wang, [3]Michael Hayes,
[4]Brendan O'Flynn, [5]Cian O'Mathuna
[1,2,3,4,5] Tyndall National Institute, Cork, Ireland
[4,5] CLARITY Center for Sensor Web Technologies, Cork, Ireland
email: wensi.wang@tyndall.ie

1 Introduction

For conventional Wireless Sensor Networks (WSN) without energy harvesting capability, chemical batteries are normally used as energy storage subsystems. In most cases, the electrochemical reactions of the battery limits the WSN system lifetime. Once the chemical is depleted, maintenance efforts must be made to either replace or recharge the battery. Given the current battery technology and power consumption of the motes, even for motes run on low duty cycle, battery replacement is required every 3-6 months [1]. For WSNs with higher power consumption or higher duty cycle, the battery may limit the motes lifetime to less than a few weeks [2]. The short lifetime of the mote becomes a severe limitation for wireless sensor networks.

By implementing energy harvesting techniques, energy in ambient sources like light, heat and vibration can be scavenged and transformed into useable form for low power WSNs, thus, the lifetime of the mote will not be limited by the available battery energy. Figure 1 shows the layout of the architecture of an indoor light energy harvesting system.

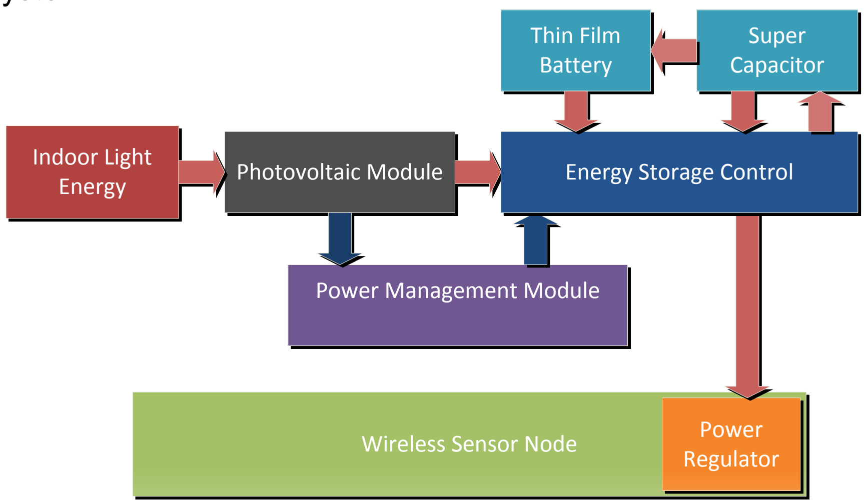

Figure 1: Energy Harvesting System Architecture

For energy harvesting powered WSNs, electric double-layer capacitors (supercapacitors) are frequently used as the energy storage [3]. With a much higher rechargeable numbers, supercapacitor enables the WSN motes being charged over a million times. Together with long shelf time, an energy harvester with supercapacitor energy storage expects 15 years operative lifetime. However, the leakage current of a supercapacitor is one order of magnitude higher than the conventional Lithium-ion battery. The energy density and capacity of the supercapacitor is also much lower than battery. The drawbacks of such lead to intensive research in more advanced supercapacitor and other alternative products.

A type of thin film lithium polymer (TFLP) battery is introduced in this paper [4]. Significantly different from conventional Lithium polymer battery, the novel design of the TFLP battery provides a high number of rechargeable cycles (>50,000 times) and low leakage alternative for the WSNs energy storage. However, the small capacity (1mAh level) and relatively high internal resistance limit the application of TFLP battery as stand-alone energy storage. Thus, a hybrid energy storage unit is proposed in this paper to create a relatively high capacity and low leakage short-to-middle term energy storage for energy harvesting powered WSNs.

In section 2, the characterization of both TFLP battery and supercapacitors are presented and analyzed. In section 3, an energy storage mathematic model is created to simulate the subsystem performance. In section 4, the hybrid energy storage unit is implemented and integrated in Tyndall mote system. The test results in real world condition are also presented and compared with supercapacitor-only energy storage.

2 Supercapacitor and Thin Film Lithium Polymer Battery

In all types of energy harvesting approaches, the energy storage subsystem is one of the key elements. WSNs powered or partly powered by an ambient energy harvester often use capacitive energy storage. Since these applications require relatively high energy density, the high capacitance electric double-layer capacitor (supercapacitor) is apparently preferred.

At the mean time, recent development of thin film Lithium polymer (TFLP) battery technologies increases the capacity of these batteries to 1 mAh level [5]. The ever increasing capacity and high number of recharge cycles make TFLP battery an attractive option for energy harvesting applications. A few energy harvesting products are now based on such technology [6].

In this work, electrical characterizations have been conducted to investigate these two different types of energy storage techniques, supercapacitor and TFLP battery. Key parameters are tested; Table I. shows the characterization results. The leakage testing results are based on data gathered in 24 hours immediately after the samples are fully charged.

The relationship between capacitance value C_E and leakage current I_{leak} is given as Leakage Correlation ρ. For the supercapacitors presented in this paper, the correlation ρ is in the range of 5-8. For supercapacitors with a capacitance higher than 2 F, the leakage current is similar to the ultra-low duty cycle average current consumption of the Tyndall mote at 20-30 μA level [7].

Table I: Energy Storages Characterization

Manu-facturer	Equivalent Capacity C_E (F)	Effective Energy Density (J/cm^3)	Average Leakage Current I_{leak} (μA)	Leakage Correlation ρ I_{leak} / Cs (μA×F^{-1})	Minimum Charging Current Ic_{MIN} (μA)	Equivalent Series Resistance R (Ω)
Maxwell	5.00	6.96	27.78	5.56	32	30
EPCOS	4.10	11.31	26.28	6.41	28	50
Cornell Dubilier	3.30	5.38	23.50	7.12	25	0.3
AVX Bestcap	0.010	0.75	0.05	5.0	1	0.1
Infinite Power Solution MEC101	4.6	130.9	0.1	0.02	1	50

In comparison, the TFLP battery IPS MEC101 shows a low leakage correlation ρ, the average leakage current over 24 hours test is only 0.1μA compare to 26.3 μA in EPCOS supercapacitor, while the TFLP battery obtains a higher capacity as well.

In the WSNs application, the Equivalent Series Resistance (ESR) of the energy storage is an important factor. Since most of the WSNs are operated in a duty cycling manner, the power consumption of a mote is 2-3 orders of magnitudes higher during the active mode than in sleep mode [8]. Energy storage with a high ESR will result in high voltage drop on the energy storage unit. The microcontroller of Tyndall mote has a lower threshold voltage at 2.5V, therefore if the voltage drop across the ESR is higher than threshold, the microcontroller will be disabled, and the data processing will not be successfully conducted. For example, the small form factor EPCOS 4.1F supercapacitor has a 50 Ω ESR and a voltage rating at 2.7V. Since the active mode current is 33.1 mA, the voltage drop on the supercapacitor is 1.65V, thus the voltage on Tyndall mote is only 1.05V. To avoid this, it is important to use low ESR energy storage to supply at least the active mode current.

3 Energy Storage Modeling

Based on the characterization, an energy storage model meant to describe the capacity, energy density, internal resistance, average leakage current, minimum charging current is created to direct the system design. Previous literature presents the physical based model and nonlinear fractional model of the supercapacitors [9] [10]. However, both of these models are not able to fully describe the characteristics of supercapacitor when μW level power is used to charge the supercapacitor.

In this paper, instead of using one physical based model, a statistic model is created to describe the supercapacitor. The model is comprised of one charging model and one discharge model based on neural networks method. The schematic of the energy storage charging model is shown in Figure 2 (a). The algorithm of the model is then trained and verified by multiple experiments conducted under same testing conditions as in the characterization tests in section 2. Similar to the charging model, the schematic of discharging model is given in Figure 2 (b).

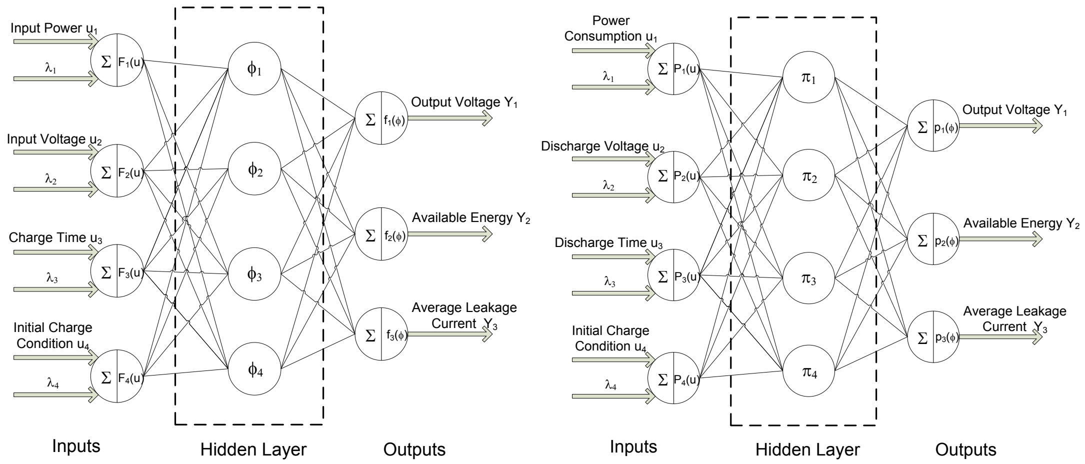

(a) (b)

Figure 2. (a) Energy Storage Charging Model (b) Energy Storage Discharging Model

In the initial phase of the learning process, a set of training data is given to create the initial weight from the inputs. The initial weight results although far away from the real condition, it sets the starting point of the learning process. In the forward pass phase of learning, inputs from training data file calculate the output based on the initial weight. The output then is compared with the target results to generate an error signal. The second phase will adjust the learning system parameters based on the learning rules. The size of adjustment step is pre-determined to avoid excessive adjustment. These two processes will repeat until the error signal reduces to lower than a defined tolerance threshold. The learning procedure is a supervised learning.

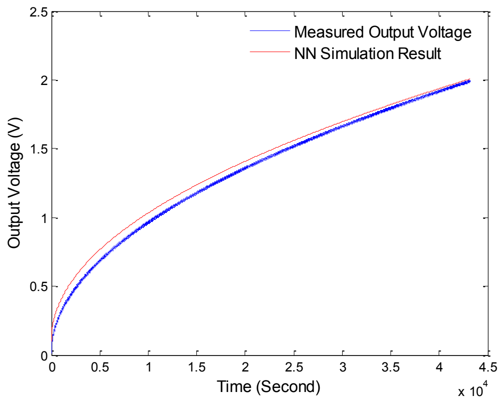

Figure 3(a)

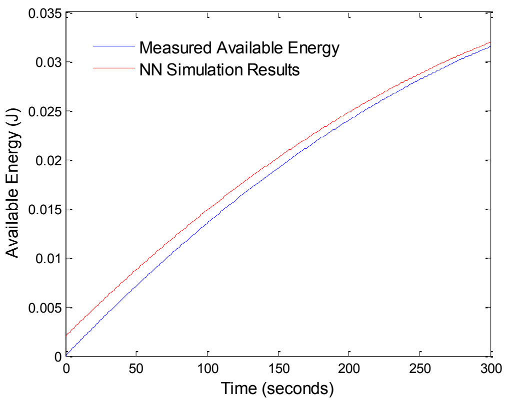

Figure 3(b)

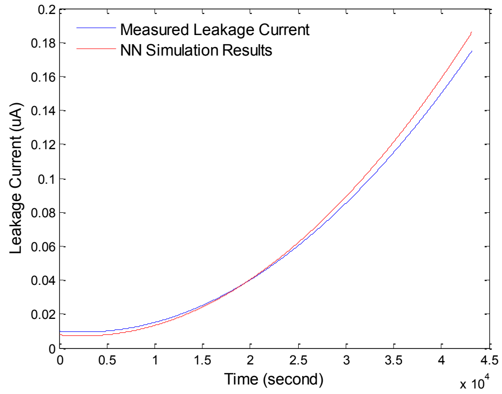

Figure 3 (c)

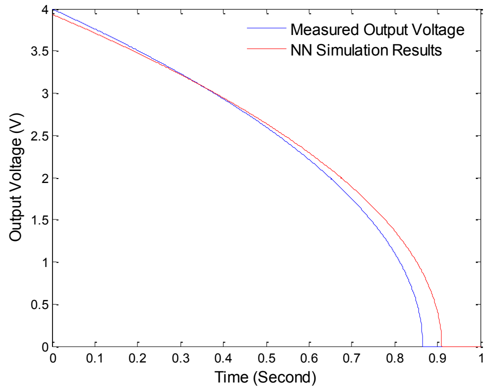

Figure 4 (a)

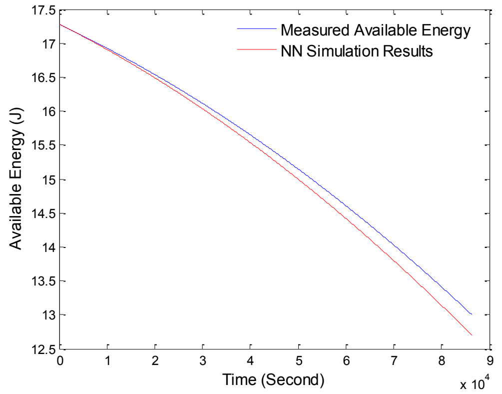

Figure 4 (b)

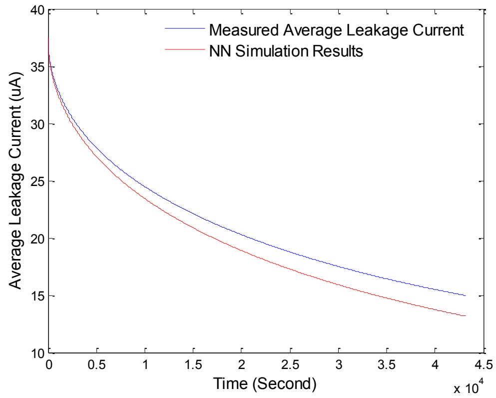

Figure 4 (c)

Three samples are chosen to create the energy storage models: Cornell Dubilier (CD) 3.3F 2.5V supercapacitor, AVX BestCap 0.01F 5V supercapacitor and IPS MEC101 1.0mAh 4.1V TFLP battery. Figure 3 (a) (b) (c) show the charging model simulation results and measured results on three samples. Figure 4 (a) (b) (c) show the discharging model simulation and measured results.

Table II. Energy Storage Model Validations shown in Figure 3 & 4

Figure Number	Charging Model	Figure Number	Discharging Model
Figure 3 (a)	CD Supercap Output voltage	Figure 4 (a)	AVX Supercap Output voltage*
Figure 3 (b)	AVX Supercap Available Energy	Figure 4 (b)	IPS TFLP Battery Available Energy**
Figure 3 (c)	IPS TFLP Battery Leakage Current	Figure 4 (c)	CD Supercap Leakage Current

Note that in Figure 4 (a), the AVX supercapacitor is discharged by active mode power consumption of a Tyndall mote. In Figure 4 (b), the IPS TFLP battery is discharged by sleep mode power consumption. For each sample, models are created based on 10 set of testing data. The tolerance threshold for the model is set to be 5%. Once the error of all 10 set of data is lower than 3%, the model is then considered to be established. Two more set of data are then used to verify the confidence of the neural network model. The results show high level of correlation between the simulation results and testing results. The error between model simulation and testing results on all samples are lower than 3.5%.

4 Modeling based Optimization and System Implementation

In energy harvesting powered WSN operation, two phases are often defined as time period T_{charge} when energy harvesting is charging the system and time period $T_{discharge}$ when energy harvesting is not available. In $T_{discharge}$ the energy used in mote is from energy storage unit. In order to maintain a continuous mote operation powered from energy harvester, two basic requirements are: first, energy harvester must charge the energy storage to required level within period T_{charge}; second, system is ability to operate while no additional energy is available for a period of time $T_{discharge}$.

Separate models are used to explain the requirement in the two phases. In the case of indoor solar energy harvesting, charging phase of the harvester module can be described with the following equation (1).

$$\overline{I_{PV}} \geq [I_{leak} + I_{act} * D + I_{sleep} * (1-D)] * (1 + \frac{V_{avg} * T_{discharge}}{\overline{V_{PV}} * T_{charge}}) \quad (1)$$

Where $\overline{I_{PV}}$ is the average PV cell output current, $\overline{V_{PV}}$ is the average PV cell output voltage, I_{leak} is the supercapacitor normalized leakage current, I_{act} is the active mode current consumption and I_{sleep} is the sleep mode current consumption. D is the duty cycle. T_{charge} is the charging time in every 24hours (average illuminance >30lux). $T_{discharge}$ is the discharge time (8hours) when illuminance <30lux, V_{avg} is the average voltage on the supercapacitor in discharge phase. The required energy consumed in the discharge phase $E_{discharge}$ is shown in the equation (2).

$$\frac{C({V_0}^2 - {V_{mote}}^2)}{2} > E_{discharge} = V_{avg} * T_{discharge} * [I_{leakage} + I_{active} * D + I_{sleep} * (1-D)] \quad (2)$$

Where C is the capacitance of the supercapacitor, V_0 is the smaller one of average PV cell output voltage and supercapacitor rated voltage. V_{mote} is the lower operational voltage limit of Tyndall mote.

By applying the NN model simulation results in Equation (1) and (2) and compare different combinations, it can be noticed that a 0.01F level supercapacitor and TFLP battery is the optimized hybrid energy storage. In active mode of mote, the 0.01F supercapacitor is used to provide the high active mode current. The low ESR gives a very low voltage drop on the supercapacitor. The short discharge time in the active mode will not discharge the supercapacitor to a voltage lower than the threshold voltage as shown in Figure 4(a). In sleep mode of the mote, the TFLP battery is used to provide a long term low leakage current power supply as shown in Figure 4 (b). The high ESR will not create a high voltage drop when the sleep mode current consumption is 7uA. In the charging phase as shown in equation (1), the TFLP battery is charged from the solar panel after maximum power point tracking. The low minimum charging current allows the TFLP battery been charged more efficiently. An external timer is used to control when to charge the supercapacitor from TFLP battery. The timer is programmed by the mote. The voltage rating of TFPL battery is higher than the Tyndall mote's required 3.0 V, while the supercapacitor's voltage can be programmed to meet the requirement. Thus, voltage regulators are only needed for the TFLP battery. The hybrid energy storage is then implemented as shown in Figure 5.

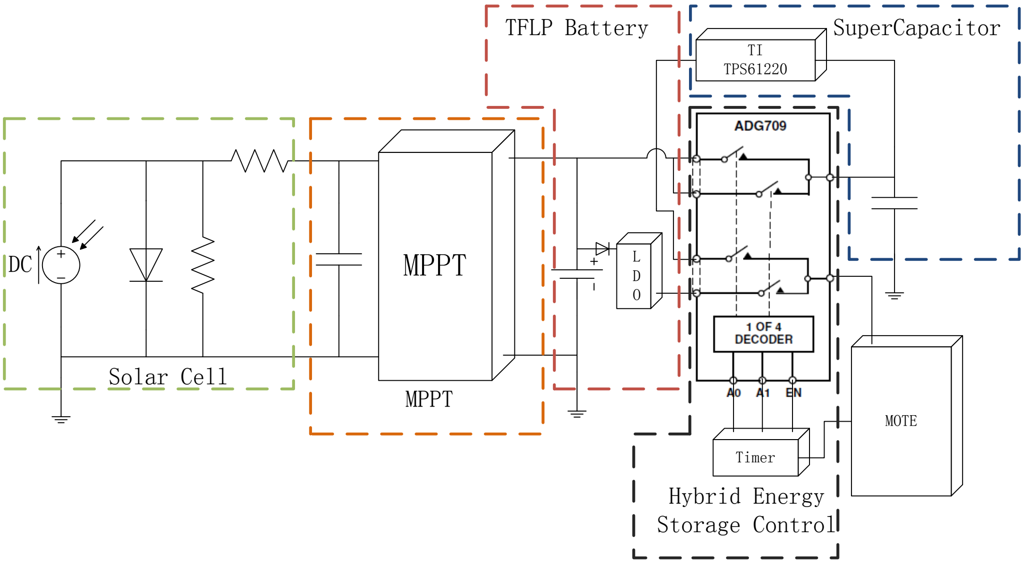

Figure 5. Hybrid Energy Storage Power Management

The proposed energy storage unit was then integrated into an indoor light energy harvesting powered WSN system shown in Figure 5 and Figure 6. The low power Tyndall WSN mote is deployed in typical office environment to measure electricity consumption data. The experimental results show that the hybrid energy storage unit enables the Tyndall WSN mote to autonomously operate continuously based on 10 hours of 350 lux indoor light illuminance every 24 hours. The proposed energy storage unit also extends the system operation lifetime in darkness by 24% from 58 hours to 72 hours.

Figure 6. Implemented Indoor Light Powered WSN with Hybrid Energy Storage

Compared to capacitive energy storage [1], the proposed hybrid energy storage solution reduces the average leakage current by 45% to 12.5 uA. The effective capacity of the energy storage is also increased 25% to 1.3 mAh.

5 CONCLUSIONS and FUTURE WORK

This paper presents the design of a hybrid energy storage solution for energy harvesting powered WSN applications. By utilizing a neural network method based energy storage system model, a 1.3 mAh hybrid energy storage unit with 4.1V voltage rating is carefully designed by taking in account all the component parameters. The testing results show that it achieves 12.5 uA low leakage current, which makes it very attractive for energy harvesting applications. By integrating the hybrid energy storage unit into the indoor light powered Tyndall WSN, it significantly extends the mote operative time in darkness by 24%. The different voltage ratings on the two types of energy storages require additional dc/dc conversion and lead to lower energy conversion efficiency. In future work, a higher efficiency dc/dc converter or other methods need to be investigated in order to further reduce the energy loss in the energy storage subsystem.

ACKNOWLEDGEMENT

This work has been funded by Scientific Foundation Ireland through research project ITOBO (398-CRP)

REFERENCES

[1] W.S. Wang, T. O’Donnell, N. Wang, M. Hayes, B. O’Flynn, C. O’Mathuna, “Design Considerations of Sub-mW Indoor Light Energy Harvesting for Wireless Sensor Systems”, ACM Journal of Emerging Technologies in Computing Systems, Volume 6, Issue 2, 2010

[2] W.S. Wang, P. Curran, N. Wang, M. Hayes, B. O'Flynn, C. O'Mathuna, “Autonomous Smart Sensing System for Building Energy Metering”, Smart System Integration 2010, Como, Italy, Mar 2010

[3] S. Saggini, F. Ongaro, C. Galperti, P. Mattavelli, "Supercapacitor-based hybrid storage systems for energy harvesting in wireless sensor networks," in *Applied Power Electronics Conference and Exposition (APEC), 2010 Twenty-Fifth Annual IEEE*, 2010, pp. 2281-2287.

[4] C. Townsend, S. Arms, M. Hamel, J. Galbreath, D. Churchill, "Thin film battery recharging from micropower energy harvesting sources," in *Applications of Ferroelectrics, 2008. ISAF 2008. 17th IEEE International Symposium on the*, 2008, pp. 1-1.

[5] Infinite Power Solution Website: www.infinitepowersolutions.com/product/thinergy

[6] Microstrain Website: www.microstrain.com/news/Thin-Film-Micro-Energy-Cells

[7] W.S. Wang, T. O’Donnell, L. Ribetto, B. O’Flynn, M. Hayes, C. O’Mathuna, "Energy harvesting embedded wireless sensor system for building environment applications," in *Wireless Communication, Vehicular Technology, Information Theory and Aerospace & Electronic Systems Technology, 2009. Wireless VITAE 2009. 1st International Conference on*, 2009, pp. 36-41.

[8] E. Jafer, B. O’Flynn, C. O’Mathuna and W.S. Wang, "Design of miniaturized wireless sensor mote and actuator for building monitoring and control," in *Telecommunications (ICT), 2010 IEEE 17th International Conference on*, 2010, pp. 887-892.

[9] L. Zubieta and R. Bonert, "Characterization of double-layer capacitors (DLCs) for power electronics applications," in *Industry Applications Conference, 1998. Thirty-Third IAS Annual Meeting. The 1998 IEEE*, 1998, pp. 1149-1154 vol.2.

[10] N. Bertrand, J. Sabatier, O. Briat, and J. Vinassa, "Embedded Fractional Nonlinear Supercapacitor Model and Its Parametric Estimation Method," *Industrial Electronics, IEEE Transactions on,* vol. 57, pp. 3991-4000, 2010.